Supporting online material for Multiscale mass-spring models of carbon nanotube foams

F. Fraternali*

Department of Civil Engineering, University of Salerno, 84084 Fisciano(SA), Italy, and Division of Engineering, King's College London, Strand, London WC2R 2LS, UK

T. Blesgen

Max-Planck-Institute for Mathematics in the Sciences, Inselstraße 22-26, D-04103 Leipzig, Germany

A. Amendola

Department of Civil Engineering, University of Salerno, 84084 Fisciano(SA), Italy

C. Daraio

Graduate Aerospace Laboratories (GALCIT) and Applied Physics, Engineering and Applied Sciences, California Institute of Technology, Pasadena, CA 91125, USA

Abstract

We present some additions to Section 5 of the article *'Multiscale mass-spring models of carbon nanotube foams'*, to be published online alongside its electronic version.

Email addresses: f.fraternali@unisa.it (F. Fraternali*), blesgen@mis.mpg.de (T. Blesgen), adamendola@gmail.com (A. Amendola), daraio@caltech.edu (C. Daraio)
*Corresponding author

Addendum to Section 5. Applications

Section 5.1. Convergence study and micromechanics of 'plastic' steps

The material properties used for the convergence study presented in Section 5.1 of the paper are given in Tab. 1.

k_0 [MPa]	$\Delta\sigma/\sigma_a$	ε_a	ε_c
50.00	-0.7	0.25	0.77

Table 1: Mechanical properties of uniform chains of microscopic bi-stable springs employed in Section 5.1 of the paper.

Section 5.2. Fitting of experimental results on compressed CNT foams

The fits presented in Section 5.2 of the paper consider single loading-unloading cycles, described by data sets of the form

$$\left\{\{\varepsilon_r - \varepsilon_0, \bar{\sigma}_r\}_{r=1,...,N_d}\right\}, \tag{1}$$

where N_d is the number of data points; $\varepsilon_1, ..., \varepsilon_{N_d}$ are experimental observations of the global strain ε (hard-device conditions); ε_0 is the permanent strain accumulated during a previous load history (mechanical preconditioning); and $\bar{\sigma}_1, ..., \bar{\sigma}_N$ are the experimental recordings of the overall stress σ. On adopting a model with N mesoscopic springs (model #2, cf. Section 5 of the paper), we look for the best-fit values of the constitutive parameters

$$\boldsymbol{p} = \left\{\left\{k_0^i,\ \Delta\sigma^i,\ k_c^i,\ \varepsilon_i^a,\ \varepsilon_c^i\right\}_{i=1,...,N}\right\}, \tag{2}$$

under simple bounds of the form

$$\boldsymbol{p} \in D = [p_1^{lb}, p_1^{ub}] \times \ldots \times [p_P^{lb}, p_P^{ub}], \tag{3}$$

Here, $P = 5N$ denotes the overall number of constitutive parameters. We reduce the independent constitutive parameters of each spring to 5 by fixing the ratios k_{h+}^i/k_0 and k_{h-}^i/k_0 (cf. Section 4 of the paper). We set $k_{h+}^i = k_0 \times 10^{-3}$ and $k_{h-}^i = k_0 \times 0.5 \times 10^{-2}$ for the first cycle of the experiment analyzed in Section 5.2.1; $k_{h+}^i = k_{h-}^i = k_0 \times 10^{-5}$ for the fourth cycle of the experiment analyzed in the same Section; and $k_{h+}^i = k_{h-}^i = k_0 \times 10^{-2}$ for the experiments analyzed in Section 5.2.2 The fitting performance of a given set of parameters $\boldsymbol{p}$ is evaluated through the fitting fitness function

$$f(\boldsymbol{p}) \;=\; \max_{r=1,\ldots,N_d} |\sigma_r(\boldsymbol{p}) \;-\; \bar{\sigma}_r| \tag{4}$$

which is the maximum-norm of the piecewise continuous residuals $\sigma - \bar{\sigma}$. Here, $\sigma_r(\boldsymbol{p})$ denotes the numerically predicted overall stress for $\varepsilon = \varepsilon_r$, coinciding at equilibrium with the stress in each individual spring. The multivariate minimization problem

$$\min_{\boldsymbol{p}\in D} f(\boldsymbol{p}), \tag{5}$$

is expected to be strongly non-convex (Ogden et al., 2004) and well suited for genetic algorithms (Schmitt, 2004; El Sayed et al., 2008). We employ the Breeder Genetic Algorithm (BGA) presented in De Falco et al. (1996) and successfully used as a parameter identification tool in Fraternali et al. (2010). We use a population size equal to $2P$; truncation selection scheme with truncation rate equal to 15%; extended intermediate recombination; mutation rate in the interval $[10\%, 50\%]$; and a maximum number of generations equal to 200. We refer the reader to De Falco et al. (1996) for further technical details of the employed BGA.

Section 5.2.1. Compression tests on a doubly anchored CNT foam

Tab. 2 illustrates the best fit material parameters obtained for the experiment illustrated in Section 5.2.1 of the paper.

Section 5.2.2. Compression tests on a foamlike CNT film

We fit the 'symmetric' formulation of model # 2 ($k_c^i = k_0^i$ in each spring) to the first cycle of the cyclic compression test given in Cao et al. (2005), employing chains with 3, 5 and 10 mesoscopic springs. The best fit parameters obtained for this case are given in Tab. 3, and the corresponding stress-strain plots are shown in Fig. 1. One observes that the matching between predictions and experimental recordings progressively increases by adding springs to the model (the fitting fitness function f decreases from 1.586 MPa to 1.462 MPa, by letting N increase from 3 to 10). A good matching between theory and experiments was also observed for what concerns the localization of the CNT deformation during the buckling ('plastic') phase. Fig. 2 shows selected equilibrium configurations and a deformation animation of the best fit model with 5 springs. It is worth noting that the succession of the spring snaps depicted in Fig. 2 qualitatively reproduces the progressive kinking of

4 springs, 1. cycle, $\varepsilon_0 = 0$, $f = 0.491$ MPa

spring #	k_0^i [MPa]	$\Delta\sigma^i/\sigma_a^i$	ε_a^i	ε_c^i	k_c^i/k_0^i
3	11.82	-0.82	0.09	0.95	9.06
2	48.89	-0.88	0.05	0.93	8.66
1	86.95	-0.75	0.06	0.61	9.58
0	16.92	-0.79	0.27	0.56	9.77

4 springs, 4. cycle, $\varepsilon_0 = 0.20$, numerical (1), $f = 0.484$ MPa

spring #	k_0^i [MPa]	$\Delta\sigma^i/\sigma_a^i$	ε_a^i	ε_c^i	k_c^i/k_0^i
3	35.93	-0.69	0.03	0.84	92.73
2	10.76	-0.98	0.88	0.88	59.37
1	20.42	-0.86	0.19	0.27	25.93
0	7.16	-0.16	0.02	0.95	96.70

4 springs, 4. cycle, $\varepsilon_0 = 0.20$, numerical (2), $f = 0.746$ MPa

spring #	k_0^i [MPa]	$\Delta\sigma^i/\sigma_a^i$	ε_a^i	ε_c^i	k_c^i/k_0^i
3	76.29	0.00	0.62	0.62	84.16
2	10.76	0.00	0.88	0.88	59.37
1	1.66	0.00	0.73	0.73	76.13
0	2.24	0.00	0.13	0.72	92.55

Table 2: Mechanical properties of 'asymmetric' spring models fitting compression tests on a doubly anchored CNT foam (cf. Section 5.2.1 of the paper).

the tubes observed during the test, which is clearly described by Figs. 1, 2 and 4A of Cao et al. (2005). The best fit parameters obtained for 'asymmetric' formulation of model # 2 (cf. Section 5.2.2 of the paper) are given in Tab. 4.

3 springs, 1. cycle, $f = 1.568$ MPa

spring #	k_0^i [MPa]	$\Delta\sigma^i/\sigma_a^i$	ε_a^i	ε_c^i
2	52.30	−0.78	0.17	0.78
1	52.30	−0.78	0.23	0.88
0	52.30	−0.78	0.27	0.73

5 springs, 1. cycle, $f = 1.512$ MPa

spring #	k_0^i [MPa]	$\Delta\sigma^i/\sigma_a^i$	ε_a^i	ε_c^i
4	45.97	−0.92	0.24	0.78
3	44.55	−0.76	0.23	0.72
2	44.58	−0.78	0.21	0.80
1	44.45	−0.76	0.30	0.84
0	47.76	−0.73	0.25	0.83

10 springs, 1. cycle, $f = 1.462$ MPa

spring #	k_0^i [MPa]	$\Delta\sigma^i/\sigma_a^i$	ε_a^i	ε_c^i
9	46.76	−0.81	0.20	0.86
8	58.04	−0.86	0.58	0.54
7	51.92	−0.80	0.25	0.87
6	48.27	−0.88	0.22	0.87
5	60.76	−0.86	0.21	0.60
4	58.10	−0.72	0.25	0.81
3	53.87	−0.70	0.18	0.80
2	44.27	−0.66	0.25	0.89
1	59.50	−0.64	0.19	0.64
0	59.73	−0.76	0.21	0.88

Table 3: Mechanical properties of 'symmetric' spring models fitting results by Cao et al. (2005).

References

Cao, A., Dickrell, P.L., Sawyer, W. G., Ghasemi-Neihad, M.N., Ajayan, P.M., (2005). Super-Compressible Foamlike Carbon Nanotube Films. Science 310, 1307-1310.

5 springs, 1. cycle, $\varepsilon_0 = 0$, $f = 0.870$ MPa

spring #	k_0^i [MPa]	$\Delta\sigma^i/\sigma_a^i$	ε_a^i	ε_c^i	k_c^i/k_0^i
4	39.06	−0.69	0.28	0.86	4.70
3	43.41	−0.65	0.31	0.81	4.71
2	48.48	−0.90	0.21	0.81	3.90
1	38.15	−0.73	0.24	0.76	5.00
0	46.89	−0.77	0.26	0.80	4.33

10 springs, 1. cycle, $\varepsilon_0 = 0$, $f = 0.808$ MPa

spring #	k_0^i [MPa]	$\Delta\sigma^i/\sigma_a^i$	ε_a^i	ε_c^i	k_c^i/k_0^i
9	45.15	−0.70	0.24	0.85	1.85
8	48.16	−0.56	0.30	0.66	5.82
7	39.88	−0.60	0.25	0.72	7.91
6	41.73	−0.61	0.19	0.76	2.70
5	54.97	−0.69	0.21	0.86	7.58
4	59.29	−0.92	0.21	0.86	2.20
3	44.24	−0.89	0.24	0.86	4.97
2	48.96	−0.79	0.27	0.88	9.68
1	61.24	−0.69	0.16	0.83	7.16
0	43.92	−0.67	0.29	0.83	6.69

5 springs, 1000. cycle, $\varepsilon_0 = 0.14$, numerical (1), $f = 0.444$ MPa

spring #	k_0^i [MPa]	$\Delta\sigma^i/\sigma_a^i$	ε_a^i	ε_c^i	k_c^i/k_0^i
4	8.66	−0.28	0.19	0.90	27.35
3	2.55	−0.27	0.74	0.74	47.35
2	86.24	−0.96	0.59	0.63	49.84
1	57.13	−0.31	0.44	0.60	20.15
0	2.95	−0.71	0.49	0.85	38.13

5 springs, 1000. cycle, $\varepsilon_0 = 0.14$, numerical (2), $f = 0.926$ MPa

spring #	k_0^i [MPa]	$\Delta\sigma^i/\sigma_a^i$	ε_a^i	ε_c^i	k_c^i/k_0^i
4	4.40	0.00	0.37	0.89	45.19
3	54.24	0.00	0.44	0.71	35.32
2	4.62	0.00	0.59	0.63	26.10
1	1.83	0.00	0.87	0.87	32.26
0	11.38	0.00	0.09	0.75	33.84

Table 4: Mechanical properties of 'asymmetric' spring models fitting results by Cao et al. (2005).

De Falco, I., Del Balio, R., Della Cioppa, A., Tarantino, E., (1996). A comparative analysis of evolutionary algorithms for function optimization. Proceedings of the Second Workshop on Evolutionary Computation (WEC2), Nagoya, JAPAN, 29-32.

El Sayed, T., Mota, A., Fraternali, F., Ortiz, M., (2008). A variational constitutive model for soft biological tissue. J. Biomech. 41, 1458-1466.

Fraternali, F., Porter, M.A., Daraio, C., (2010). Optimal design of composite granular protectors. Mech. Adv. Mat. Struct., 17, 1-19.

Ogden, R.W., Saccomandi, G. , Sgura, I., (2004). Fitting hyperelastic model to experimental data. Comput. Mech 34(6), 484-502.

Schmitt, L.M.,(2004). Theory of Genetic Algorithms II: models for genetic operators over the string-tensor representation of populations and convergence to global optima for arbitrary fitness function under scaling. Theor. Comput. Sci. 310(1-3), 181-231.

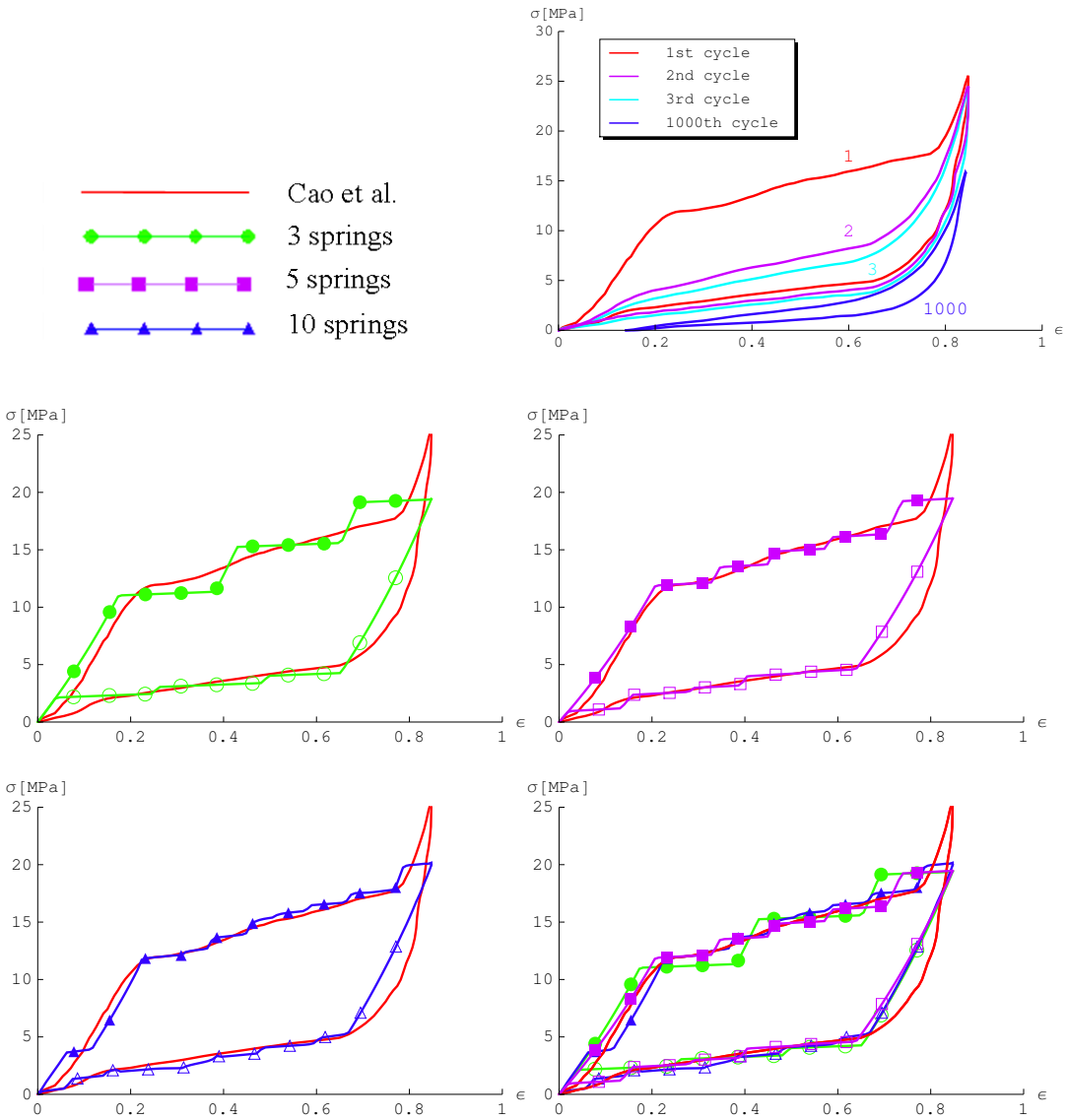

Figure 1: (Fitting of the first cycle of a compression test on a foamlike CNT film to non-uniform spring models (properties in Tab. 3).

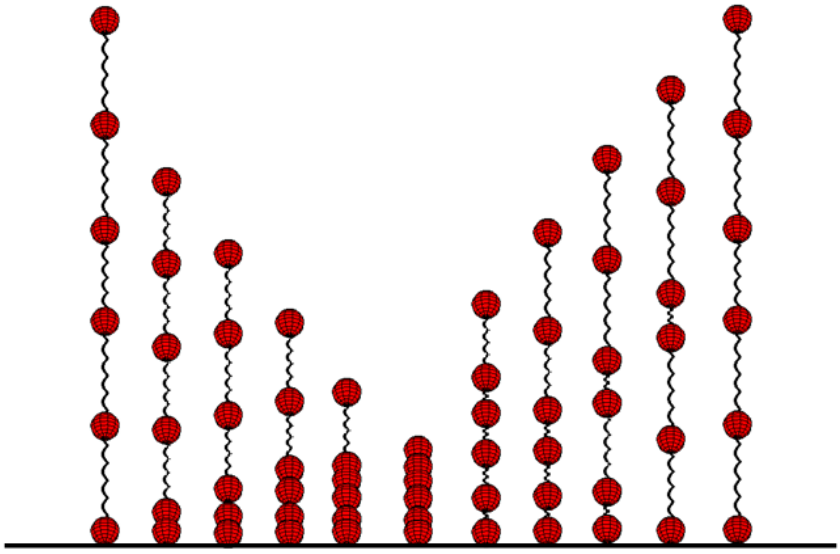

(animation)

Figure 2: Selected equilibrium configurations (left) and deformation animation (right) of the model with five springs described in Tab. 3.